EVALUATING EROSION FROM SPACE: A CASE STUDY NEAR UBERLÂNDIA

Anton Vrieling[1]
Silvio C. Rodrigues[2]
Geert Sterk[1]

[1] Wageningen University, Erosion and Soil & Water Conservation Group, Wageningen, The Netherlands, Email: anton.vrieling@wur.nl - geert.sterk@wur.nl
[2] Universidade Federal de Uberlândia, Instituto de Geografía, Uberlândia MG, Brazil, Email: silgel@ufu.br

ABSTRACT

Satellites can offer important spatial data for the assessment of soil erosion. This study was conducted to explore how satellite imagery could be used for evaluating erosion in a 10*10 km area in the Brazilian Cerrados. Products obtained from a variety of satellite sensors were analyzed for the purpose of (1) detecting erosion features; and (2) qualitatively mapping erosion risk. Erosion detection was done through visual image interpretation. Optical Terra ASTER images allowed for a better detection and delineation of major gullies as ENVISAT ASAR imagery. Gully dynamics could be assessed by jointly interpreting aerial photos of 1979 and a high-resolution QuickBird image of 2003. QuickBird also allowed for the detection of smaller erosion features, like rills. Erosion risk mapping was performed for the complete study area with a simple qualitative method integrating information on slope and vegetation cover. Slope was calculated from the SRTM DEM, and NDVI, being indicative of vegetation cover, was obtained from a wet-season ASTER image. Both factors were automatically classified based on their relative susceptibility to erosion. The erosion risk map was constructed by combining both classifications with the minimum-operator. The accuracy of the map was good (75 %) when compared to field estimates of erosion risk. The method presented therefore allowed for a quick and proper indication of spatial differences of erosion risk in the study area, particularly concerning rill and sheet erosion.

INTRODUCTION

Space technology is becoming an increasingly important tool in human lives. Many satellites are currently in orbit around the earth. They are used for communication, navigation, earth observation, and scientific exploration of the universe. For land degradation studies, systems of interest include the Global Positioning System (GPS) and earth observing systems. GPS

allows for a quick determination of the location where measurements and surveys are being made. Earth observing systems allow for a regular inventory of the earth's surface at different spatial and temporal scales. Important spatial information on physical variables can be derived from sensors onboard satellites, providing frequent imagery. For land degradation studies, such information is generally difficult to obtain from other sources, especially for large areas.

The most important land degradation problem worldwide is soil erosion by water (Eswaran et al., 2001). Agricultural production, infrastructures, and water quality can become severely influenced by erosion processes causing strong environmental impacts and high economic costs (Lal, 1998; Pimentel et al., 1995). Soil erosion processes by water can be divided into: *splash erosion*, which occurs when soil particles are detached and transported as a result of the impact of falling raindrops; *sheet erosion*, which removes soil in layers and is caused by the combined effects of splash erosion and surface runoff; *rill erosion*, which is the disappearance of soil particles caused by concentrations of flowing water; and *gully erosion*, that occurs when the flow concentration becomes large and the incision deeper and wider than with rills. Gully dynamics are however not limited to fluvial processes only, but are greatly influenced by sub-surface flow, tunneling and side-wall failures (Bocco, 1991).

Spatial data are required for the assessment of erosion. Satellite data can play an important role, both for the detection of erosion features and eroded surfaces, and for the assessment of erosion determining factors like topography and vegetation cover (Vrieling, 2004). Starting in 1972 with the launch of Landsat-1, satellite imagery has become increasingly available. Current spaceborne sensors provide imagery with spatial resolutions going down to less than a meter (QuickBird). Moreover, image costs have gone down substantially, which opens the use of remote sensing imagery to a wider public. At present, a lot of cheap or free satellite data are available from the internet, including optical images (e.g. Terra ASTER), and digital elevation models such as the Shuttle Radar Topography Mission (SRTM) DEM (Rabus et al., 2003).

The objective of this study is to explore the potential use of satellite imagery for assessing erosion within a 10*10 km area in the Brazilian Cerrados.

Study area

The 10*10 km study area is located near the city of Uberlândia, in the Cerrados region of Brazil (Figure 1). The Cerrados cover about 25% of Brazil's territory. This natural savanna ecosystem originally consisted of grassland, shrubland, and woodland (Furley, 1999). During the past 30 years the ecosystem has experienced important impacts from the expansion of agriculture, cattle raising and forestry. Approximately 40% of the Cerrado area has been converted to human land uses (Ferreira and Huete, 2004). A major negative environmental impact of these land conversions has been soil erosion (Rodrigues, 2002).
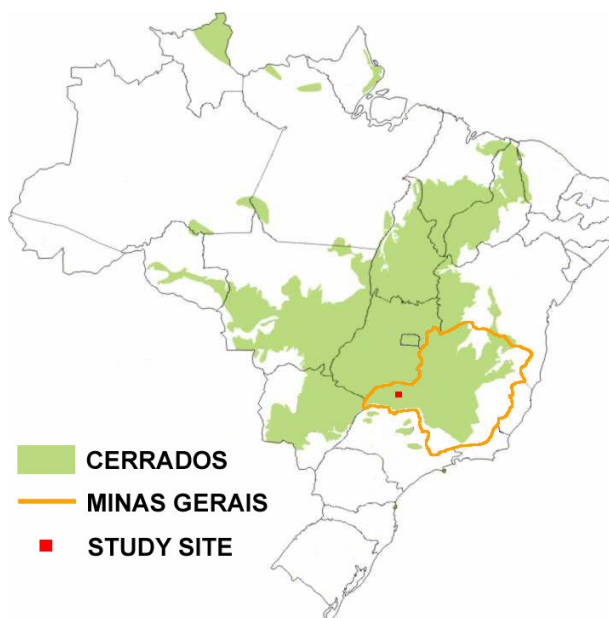
Figure 1. Location of study site within the Brazilian Cerrados

The study area has a humid tropical climate with an average annual rainfall of 1,500 mm/year. Rainfall occurs between October and April, with highest amount and intensities during the months December-February. The months May to September are rather dry. Topography is slightly undulating with slopes between 0 and 15 %, and heights ranging from 700 to 900 m above mean sea level. Most soils in the area consist of loamy sand, and are generally deep, with soil depths of up to 25 m.

The vegetation cover consists mainly of pastures. Many pastures are degraded, which implies a high fraction of weeds and shrubs, and a relatively limited vegetative ground cover. Scattered trees and shrubs occur to different extents within the pastures. Sometimes degraded pastures are renovated, which implies cutting and burning of present weeds, shrubs, and trees,

685

resulting in a bare soil for several months. There is a gradual transition from pastures to shrubland and woodland. Gallery forest occurs along the main drainage lines.

Several huge gullies of up to 25 m deep and more than 100 m wide are present in the area. These gullies probably initiated due to increased drainage by road construction, parceling of properties by didges, and land conversions. Most gullies are more than 50 years old, although some smaller gullies occur of more recent origin. Less apparent erosion forms are sheet and rill erosion. These are the result of limited infiltration on crusted soils. Crusting takes place due to the impact of rainfall on unprotected soil. Runoff therefore increases and entrains detached sediments. This process is somewhat controlled by constructed earthen contourbunds of about 0.50 to 1.00 m high, causing sedimentation of soil particles behind the bund. Nevertheless, bad maintenance and poor construction often worsens the situation, due to concentration of water and subsequent ruptures in the bunds. This can even trigger gully formation or gully advance in some cases.

MATERIALS AND METHODS

Data

Remote sensing data sources used in this study included:
1. Two Terra ASTER images acquired on 4 March and 11 August 2003 (15-m resolution in three spectral bands)
2. Three ENVISAT ASAR imagery (HH polarization) acquired on 13 January, 28 April, and 7 July 2003 (30-m resolution and 12.5-m pixel size)
3. A panchromatic QuickBird image acquired on 4 August 2003 (0.6-m resolution)
4. Aerial photos acquired on 21 April 1979 (about 2-m resolution)
5. An SRTM C-band DEM (90-m resolution)

Fieldwork was done from December 2003 till February 2004, and included an assessment of gully characteristics and the execution of a field survey. A total of 356 locations throughout the area were visited during the survey, for which the following characteristics were recorded: co-ordinates (GPS), land cover, fractional vegetation cover, presence and state of contourbunds, slope inclination, and erosion indicators. Erosion risk was qualitatively estimated on a scale ranging from 1 (very low) to 5 (very high), based on the recorded surface

686

characteristics and the presence of erosion indicators. Used indicators of high erosion risk included presence of rills and gullies, signs of overland flow, exposed roots, ruptures in contourbunds, and the presence of strong crusts. Furthermore, several points were taken by the GPS on road intersections for georeferencing purposes.

Pre-processing

Prior to image analysis, all the images were corrected to obtain a proper geometry and allow their overlay. This was done in several steps. First, the QuickBird image was orthorectified using the SRTM DEM to remove geometric image distortions caused by the terrain. The geometry of the orthorectified QuickBird image was subsequently corrected using the georeferencing points taken in the field. This resulted in a good positional accuracy of less than 10-m. For the aerial photos a similar procedure was followed.

ASTER images were obtained as surface reflectance products, which are corrected for atmospheric influences. Geo-referencing was done through the identification of similar points compared to the corrected QuickBird image. A first order polynomial model was used to convert the imagery to the correct geometry. A cubic convolution resampling to a 12.5-m pixel size was performed, which is the same pixel size as the ENVISAT ASAR (Advanced Synthetic Aperture Radar) imagery.

ENVISAT ASAR imagery were calibrated resulting in the backscattering coefficient normalized by the radar incidence angle (γ^0), expressed in dB. Speckle was reduced through the application of a Gamma MAP filter (Shi and Fung, 1994) applied on a 3*3 window. Because the polynomial model did not result in a good overlay with other images, the Delaunay triangulation method was applied.

Image analysis and erosion risk mapping

To explore the potential for erosion assessment using satellite imagery, two possibilities exist: (1) the direct detection of erosion features, and (2) the assessment of erosion determining factors. The direct detection of erosion was done through the visual interpretation of the imagery. By comparing different image types, the type allowing for the best visual discrimination of erosion features could be identified. To assess temporal changes in gully extent, the high-resolution QuickBird image was compared with the aerial photos. QuickBird was also used to assess smaller erosion features.

687

Erosion detection is only possible for features of sufficient spatial size. Nevertheless, even for large areas it is possible to construct maps of erosion risk. Such maps indicate where erosion is likely to occur. They can be constructed through the integration of spatial data on erosion determining factors, using models or qualitative approaches. These data can be derived from satellite imagery (Vrieling, 2004). Here a simple qualitative method presented by Vrieling *et al.* (2005) is applied to the study area, which uses the SRTM DEM and a wet-season ASTER image of 4 March 2003.

The SRTM DEM was used to calculate slope. The resulting slope map was converted to a 12.5-m grid using a cubic convolution resampling. From the ASTER image, the Normalized Difference Vegetation Index (NDVI) was calculated using the following equation:

$$NDVI = \frac{\rho(NIR) - \rho(red)}{\rho(NIR) + \rho(red)} = \frac{\rho(band\,3) - \rho(band\,2)}{\rho(band\,3) + \rho(band\,2)} \tag{1}$$

where ρ stand for reflectance. For healthy green vegetation $\rho(NIR)$ is high, while $\rho(red)$ is low, resulting in a high NDVI, whereas for bare soil $\rho(NIR)$ and $\rho(red)$ are similar causing a low NDVI. Therefore this index relates to the fractional cover and the status of the vegetation present. Both the NDVI-values and slope-values were automatically classified into five classes occupying an equal area within the study area. For both factors, an erosion risk class (five classes ranging from very low - 1 to very high - 5) was assigned based on the relative erosion susceptibility. For instance, the steepest slope class obtained a very high factorial erosion risk class, whereas flat areas and very gentle slopes received a very low risk class. For NDVI it was the other way around, i.e. very high NDVI values obtained a very low risk class. The erosion risk map was constructed by simply taking the minimum of the NDVI-based and the slope-based risk classes at each location. The minimum-operator was chosen because it was assumed that the lowest of the two factorial risk classes is determinative for the final erosion risk, because e.g. a good vegetation cover on a steep slope and a poor cover on a very gentle slope both result in a relatively little erosion.

To assess the accuracy of the erosion risk maps, the 356 field estimates of erosion risk were compared against mapping results for the same locations. The frequency of occurring combinations of estimates and mapping results were tabulated in a confusion matrix. From the

688

confusion matrix a quantitative measure of accuracy (A) was calculated. This measure defined a correct classification as one which has not more than a one-class difference from the field estimate of erosion risk. A one-class difference may be acceptable because classes are not defined on a nominal scale, but on an ordinal scale. Accuracy is then the sum of points with a maximum of one-class difference, divided by the total number of points.

RESULTS AND DISCUSSION

Erosion detection

Several gullies in the study area have large spatial sizes. Therefore satellite images allow for the detection of these features. The image resolution and imaging principles are very important for the detection possibilities. Figure 2 presents several images of a major gully in the study area of different image types. It is obvious that the QuickBird image (Figure 2d) best represents the gully extent due to its high resolution (0.6-m). However, to analyze the occurrence and distribution of gullies in a large area, this image type is not optimal due to (1) high image costs, and (2) the large amount of data. Figure 2a shows an ENVISAT ASAR image. The high backscatter (white areas) is caused by lay-over and double-bounce effects due to the steep gully sidewalls. Therefore, gully detection is possible with SAR imagery. Nevertheless, there is a high variation between images from different dates, as becomes clear from Figure 2b. The ASTER image (Figure 2c) provides a much better delineation of the gully. The gully shows distinct spectral features from its surroundings, partly due to the high presence of bare soil, partly because of shadows.
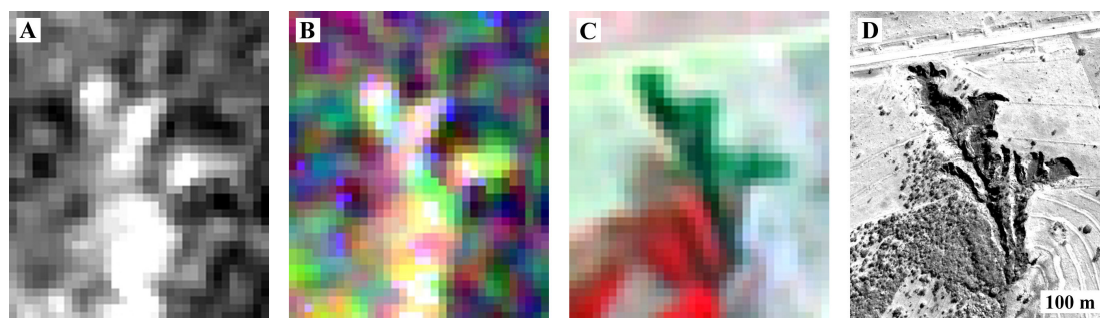
Figure 2. Several images of the same gully: (a) ENVISAT ASAR of 7 July 2003; (b) ENVISAT ASAR composite of July, April, and January 2003; (c) ASTER false color composite of 11 August 2003; (d) QuickBird image.

The possibility of detecting gullies with SAR imagery also depends highly on the orientation of the gully walls. SAR is an active system that transmits microwaves in a specific direction under a certain angle. Figure 3 shows a comparison of ASTER and ENVISAT (same

689

characteristics of the composite as Figure 2b) for a larger part of the study area having a large number of gullies. North-south oriented gully walls are clear on Figure 3a, which in this case is mostly caused by radar shadows (resulting in dark lines). However, parts of gully systems with a different orientation cannot be detected (e.g. gully 1, 2, and 4), whereas gully 3 cannot be seen at all on the ENVISAT composite and gully 5 hardly. The ASTER image (Figure 3b) shows a lot clearer where the gullies are located, and it gives a good delineation of the gully limits. Based on the distinct spectral properties of the gullies, there is a potential to automatically detect gully locations for large areas within the Brazilian Cerrados using unsupervised or supervised classification techniques on dry season ASTER imagery.
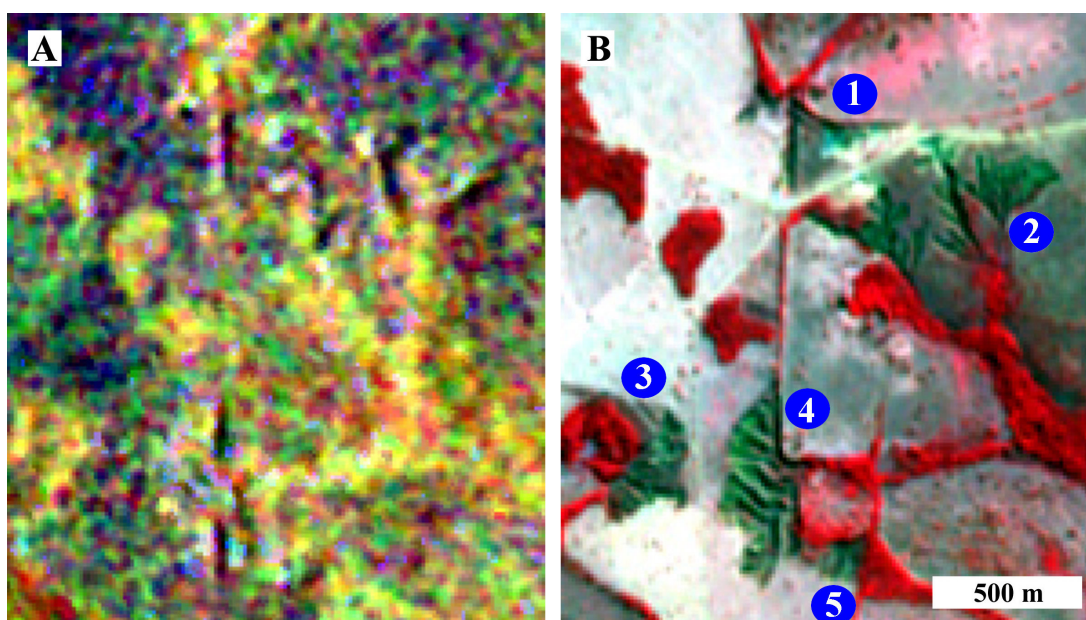
Figure 3. Part of study area with many large gully systems displayed as ENVISAT ASAR composite and ASTER false color composite.

To assess the retreat of gullies, the resolution of ASTER or ENVISAT SAR images is not sufficient. Potentially, an indication of gully retreat may be obtained from two ASTER images. However, ASTER still has a limited data archive because the Terra satellite (with ASTER onboard) was launched in 1999. A method that others have used for assessing gully retreat is the comparison of aerial photos of different years (e.g. Vandekerckhove et al., 2003). High-resolution satellite imagery can play a similar role. Figure 4 shows a comparison of the aerial photographs of 1979 and the QuickBird image of 2003 for an active gully in the study area. The gully has experienced a significant retreat in different directions. The linear retreat

of the gully head is about 70-m, or about 3 m/year. However, the retreat of gullies is not gradual over the years, but is triggered by major rainfall events, or sudden changes in the landscape changing the natural equilibrium. The major gully head is currently an important menace to the road. The eastern digits of the gully were negatively affected by the construction of contourbunds. Water could concentrate behind them and entered straight into the gully, which becomes clear of the gully retreat just upstream of the contourbunds at locations 1 and 2 (Figure 4b).
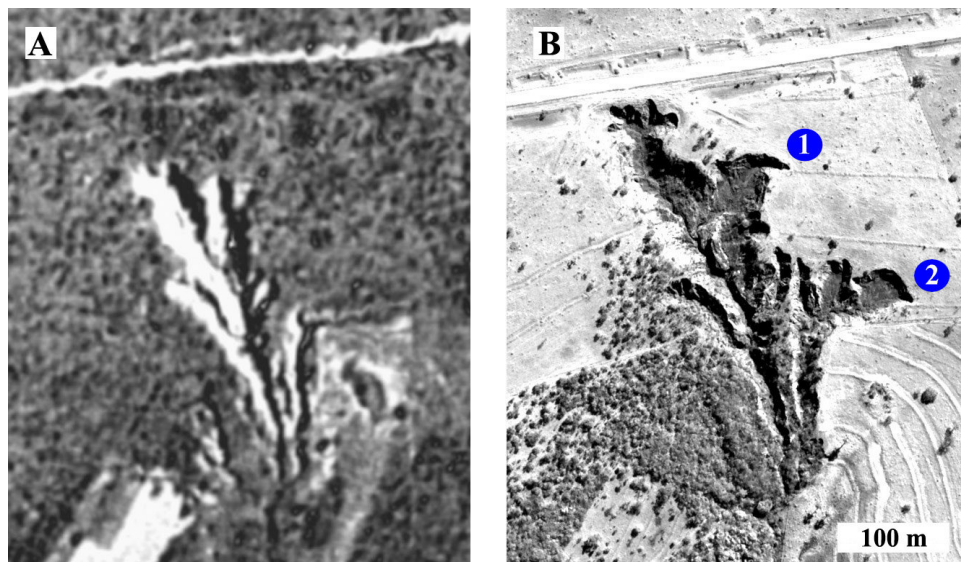
Figure 4. Active gully as seen from (a) aerial photographs of 1979, and (b) QuickBird image of 2003.

Within the study area, people have tried actively to control some of the gullies. Figure 5a shows an active gully which in 1979 was forming a major problem to the principal road. On Figure 5b an important part of the gully has disappeared. The field survey and interviews made clear that the gully was filled with waste from the city, which consisted partly of construction waste but also of domestic waste. The waste was covered with sand and structures to divert runoff water were constructed. Although gully control seems to have been effective, a large negative effect on groundwater quality can be expected. In several other large gullies in the area old car tires have been dumped, which did not result in effective gully control.
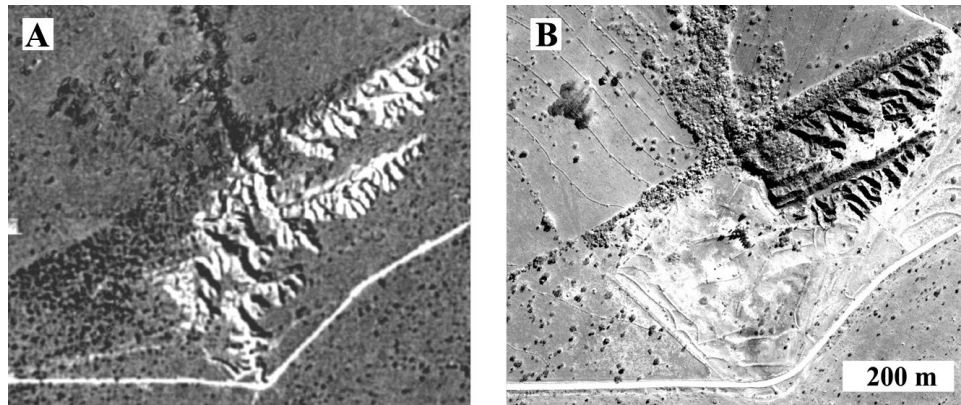
Figure 5. Recuperated gully as seen from (a) aerial photographs of 1979, and (b) QuickBird image of 2003.

Besides the analysis of large gullies, QuickBird imagery also allows the assessment of smaller erosion features. Figure 6 shows the result of runoff concentration, which may partly be attributed to the dirt road on the left of the image. The first part downstream of the road is unprotected by contourbunds, which results in an increase of concentrated flow. The concentration of water that arrives behind the first contourbunds becomes too large, and causes a rupture. This results in a chain-reaction of failures downstream. Most of the failures were repaired at the moment the image was taken, but it is likely that run-off will concentrate again along the same flow patterns and cause ruptures. These concentrated flow patterns can potentially develop into gullies.
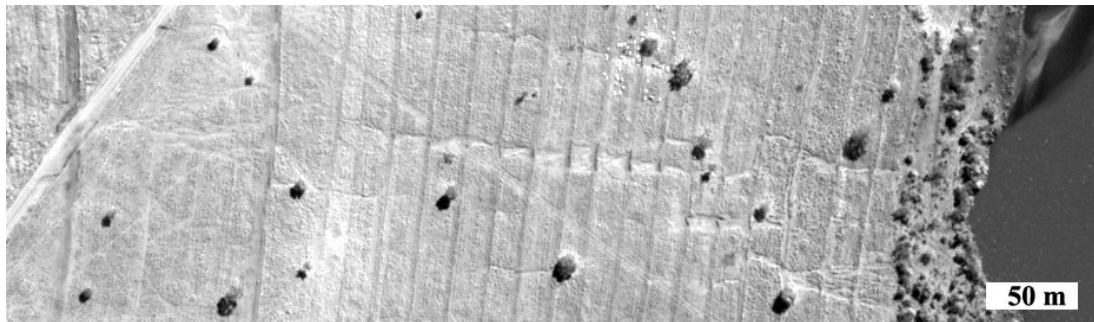
Figure 6. QuickBird image showing concentrated runoff resulting in rill erosion. Failure of contourbunds is due to concentration of water behind the bunds. Most failures were subsequently repaired.

Erosion risk mapping

The NDVI was calculated from the ASTER image (Figure 7a) and classified into five equal frequency classes (Figure 7c). From the SRTM DEM (Figure 7b), five slope classes were derived (Figure 7d) which also have an equal frequency of occurrence. The class limits for both factors are presented in Table I, and based on the relative susceptibility of erosion an

692

erosion risk class was assigned. The erosion risk map (Figure 7e) was created by taking the minimum value of Figure 7c and 7d for each location. Relatively flat areas between drainage lines and river valleys with gallery forest showed a very low erosion risk. The highest erosion risk was found on steeper slopes with limited vegetation cover at the time of image acquisition. These areas are mostly situated near the drainage lines. The mapping results mostly relate to sheet and rill erosion risk. Gullies were not effectively identified due to the complex nature of gully erosion processes and therefore the causative factors responsible for its occurrence (Baccaro, 1999; Bocco, 1991). However, at locations indicating a high erosion risk new gullies may initiate.
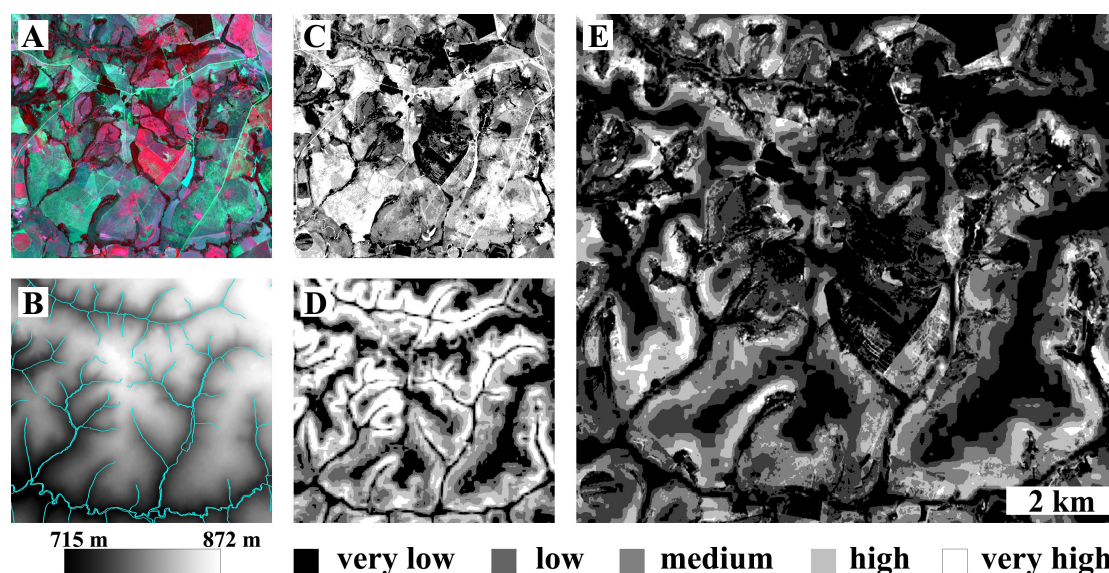
Figure 7. Erosion risk mapping for the complete study area: (a) ASTER false color composite of 4 March 2003; (b) SRTM DEM with blue lines representing drainage network digitized from topographic map; (c) ASTER-derived NDVI classes; (d) SRTM-derived slope classes; and (e) erosion risk map.

Table I. Factorial erosion risk classes based on equal frequency of each class.

Factorial erosion risk classes	NDVI range	slope range
very low (1)	> 0.782	< 3.09
low (2)	0.715 – 0.782	3.09 – 4.47
medium (3)	0.656 – 0.715	4.47 – 5.78
high (4)	0.591 – 0.656	5.78 – 7.58
very high (5)	< 0.591	> 7.58

Table II presents the confusion matrix comparing 356 field estimates of erosion risk with the classification results for the same locations. The accuracy calculated from this matrix was 75

693

% when allowing a one-class difference. This value can be considered quite good, and therefore the method presented allows for a proper identification of areas with low and high erosion risk within the study area. A factor that limits the accuracy value obtained is the fact that the fieldwork was executed a year after the ASTER image acquisition. Although both were situated in the wet season, several recent changes had occurred during that year, like the clearing of vegetation in certain areas. This caused higher field estimates of erosion risk as what could be expected from the 2003 situation recorded by ASTER. These points should ideally be discarded for the accuracy assessment, but for the current analysis it was chosen to use all points to obtain a conservative accuracy estimate.

Table II. Confusion matrix for validation of the erosion risk map.

		Field estimate of erosion risk					
		Very low	Low	Medium	High	Very high	Total
Erosion risk map	Very low	29	46	21	9	2	107
	Low	16	44	19	9	9	97
	Medium	6	27	27	6	9	75
	High	3	16	16	13	16	64
	Very high	1	1	2	4	5	13
	Total	55	134	85	41	41	356

For the mapping of erosion risk, vegetation dynamics were not taken into account. These can however have an important impact on the results, because strong seasonal dynamics exist in the study area which depend on the vegetation type (Vrieling and Rodrigues, 2004). For the static analysis presented here, the image timing can be important. Ideally the satellite image is acquired at the moment when a lot of erosion can be expected. This is often during the beginning of the rainy season, when vegetation cover is still limited, whereas heavy and intense rainfall occurs. A problem is however the frequent cloud cover. SAR is not limited by cloud cover, but is less effective in providing a measure of vegetation cover with small ambiguity, due to the important influence of other factors like soil moisture and vegetation height on the returned signal. Therefore, the ASTER image of March 2003 was selected as an optimal solution. It is possible that differences in the results remain limited when selecting a differently timed image, e.g. of August 2003, because NDVI classes are assigned based on occurring values. This point would need further investigation.

CONCLUSIONS

Major gullies could be properly identified for large areas in the Brazilian Cerrados using dry-season Terra ASTER imagery. ENVISAT ASAR imagery performed worse than ASTER in the detection and delineation of gullies. Therefore, for large areas of the Brazilian Cerrados dry-season ASTER imagery may allow the quick detection of gullies. A detailed assessment of gully dynamics was achieved through the combined visual interpretation of both high-resolution QuickBird imagery and aerial photographs. Smaller erosion features could also be effectively identified with QuickBird imagery, and the image analysis gave insight in the occurring processes.

The qualitative integration of the NDVI and slope provided a good indication soil erosion risk within the study area, particularly concerning rill and sheet erosion. Information on these factors could be easily obtained from a limited amount of readily including an SRTM DEM and an ASTER image. Timing of the satellite image is an important issue for accurate erosion risk assessment and potentially has a high influence on the results.

REFERENCES

Baccaro, C.A.D., 1999. Processos erosivos no Domínio do Cerrado. In: A.J.T. Guerra, A.S.d. Silva and R.G.M. Botelho (Editors), Erosão e Conservação dos Solos. Bertrand Brasil, Rio de Janeiro, Brazil, pp. 195-227.

Bocco, G., 1991. Gully erosion: processes and models. Progress in Physical Geography, 15(4): 392-406.

Eswaran, H., Lal, R. and Reich, P.F., 2001. Land degradation: an overview. In: E.M. Bridges et al. (Editors), Response to land degradation. Science Publishers Inc., Enfield, NH, USA, pp. 20-35.

Ferreira, L.G. and Huete, A.R., 2004. Assessing the seasonal dynamics of the Brazilian Cerrado vegetation through the use of spectral vegetation indices. International Journal of Remote Sensing, 25(10): 1837-1860.

Furley, P.A., 1999. The nature and diversity of neotropical savanna vegetation with particular reference to the Brazilian cerrados. Global Ecology and Biogeography, 8(3-4): 223–241.

Lal, R., 1998. Soil erosion impact on agronomic productivity and environment quality. Critical Reviews in Plant Sciences, 17(4): 319-464.

Pimentel, D. et al., 1995. Environmental and economic costs of soil erosion and conservation benefits. Science, 267: 1117-1123.

Rabus, B., Eineder, M., Roth, A. and Bamler, R., 2003. The shuttle radar topography mission: a new class of digital elevation models acquired by spaceborne radar. ISPRS Journal of Photogrammetry and Remote Sensing, 57(4): 241-262.

Rodrigues, S.C., 2002. Impacts of human activity on landscapes in Central Brazil: a case study in the Araguari watershed. Australian Geographical Studies, 40(2): 167-178.

Shi, Z. and Fung, K.B., 1994. A comparison of digital speckle filters, Proceedings of IGARSS'94. IEEE, Pasadena, California, pp. 2129-2133.

Vandekerckhove, L., Poesen, J. and Govers, G., 2003. Medium-term gully headcut retreat rates in Southeast Spain determined from aerial photographs and ground measurements. Catena, 50(2-4): 329-352.

Vrieling, A., 2004. Satellite remote sensing for water erosion assessment: a review. Catena, submitted.

Vrieling, A. and Rodrigues, S.C., 2004. Erosion assessment in the Brazilian Cerrados using multi-temporal SAR imagery, Proceedings of ENVISAT Symposium. ESA, Salzburg, Austria.

Vrieling, A., Sterk, G. and Vigiak, O., 2005. Spatial evaluation of soil erosion risk in the West Usambara Mountains, Tanzania. Land Degradation and Development, submitted.